Current Optics and Photonics
Vol. 1, No. 1, February 2017, pp. 51-59

ISSN: 2508-7266(Print) / ISSN: 2508-7274(Online)
DOI: https://doi.org/10.3807/COPP.2017.1.1.051

Non-ablative Fractional Thulium Laser Irradiation Suppresses Early Tumor Growth

Su Woong Yoo[1], Hee-Jin Park[2], Gyungseok Oh[2], Soonjoo Hwang[1], Misun Yun[3], Taejun Wang[4], Young-Seok Seo[5], Jung-Joon Min[3], Ki Hean Kim[4], Eung-Sam Kim[6], Young L. Kim[7], and Euiheon Chung[1,2]*

[1]Department of Biomedical Science and Engineering, Institute of Integrated Technology (IIT), Gwangju Institute of Science and Technology (GIST), Gwangju 61005, Korea
[2]School of Mechanical Engineering, Gwangju Institute of Science and Technology (GIST), Gwangju, 61005 Korea
[3]Department of Nuclear Medicine, Chonnam National University Medical School and Hwasun Hospital, Jeonnam 58128, Korea
[4]Division of Integrative Biosciences and Biotechnology, Pohang University of Science and Technology, Gyeongbuk 37673, Korea
[5]R & D center, WONTECH Co., Ltd., Daejeon 34028, Korea
[6]Department of Biological Sciences, Chonnam National University, Gwangju 61186, Korea
[7]Weldon School of Biomedical Engineering, Purdue University, IN 47907, USA

(Received December 15, 2016 : revised December 23, 2016 : accepted December 26, 2016)

In addition to its typical use for skin rejuvenation, fractional laser irradiation of early cancerous lesions may reduce the risk of tumor development as a byproduct of wound healing in the stroma after the controlled injury. While fractional ablative lasers are commonly used for cosmetic/aesthetic purposes (e.g., photorejuvenation, hair removal, and scar reduction), we propose a novel use of such laser treatments as a stromal treatment to delay tumorigenesis and suppress carcinogenesis. In this study, we found that non-ablative fractional laser (NAFL) irradiation may have a possible suppressive effect on early tumor growth in syngeneic mouse tumor models. We included two syngeneic mouse tumor models in irradiation groups and control groups. In the irradiation group, a thulium fiber based NAFL at 1927 nm was used to irradiate the skin area including the tumor injection region with 70 mJ/spot, while no laser irradiation was applied to the control group. Numerical simulation with the same experimental condition showed that thermal damage was confined only to the irradiation spots, sparing the adjacent tissue area. The irradiation groups of both tumor models showed smaller tumor volumes than the control group at an early tumor growth stage. We also detected elevated inflammatory cytokine levels a day after the NAFL irradiation. NAFL treatment of the stromal tissue could potentially be an alternative anticancer therapeutic modality for early tumorigenesis in a minimally invasive manner.

Keywords : Non-ablative fractional laser, Tumor growth suppression, Early cancer therapy
OCIS codes : (170.2655) Functional monitoring and imaging; (170.3880) Medical and biological imaging; (140.3460) Lasers; (170.1870) Dermatology

I. INTRODUCTION

Fractional laser resurfacing is a minimally invasive treatment that delivers small doses of laser light to biological tissue. It is typically used for photorejuvenation of aged skin. It thermally damages microscopic columns of epidermal and dermal tissue in a controlled manner over a fraction of the skin surface at regularly spaced spots [1, 2]. Both ablative fractional laser (AFL) and non-ablative fractional laser (NAFL) irradiation are well-established methods to repair photoaged

*Corresponding author: ogong50@gist.ac.kr
Color versions of one or more of the figures in this paper are available online.

skin. While AFL irradiation removes the entire epidermis of the treatment area, NAFL irradiation methods can be used for delivering a controlled dermal injury [3, 4]. Because of the intact tissue surrounding each irradiated tissue column, compared with AFL irradiation, there is rapid healing and less downtime when NAFL irradiation is used.

Moreover, AFL irradiation of precancerous lesions can reduce the risk of cancer occurrence in non-melanoma skin cancer (NMSC) as a byproduct of wound healing after the controlled injury [5, 6]. By replacing geriatric keratinocytes with newly developed ones, the risk of NMSC developing from the precancerous lesion may be decreased. Photoablation, including photodynamic therapy for actinic keratosis in the skin, Barrett's esophagus, and other gastrointestinal tumors, has been useful for patients with dysplasia and even early cancer. Reepithelialization after laser skin resurfacing can decrease the rate of skin cancer in high-risk patients [7]. Laser ablation treatments for Barrett's esophagus can also result in reepithelialization with squamous regeneration [8]. However, these methods strongly suggest that the simple removal of dysplastic epithelia is insufficient. Renormalization of sustained stromal or subepithelial signals (i.e. tissue microenvironments) is important to delay or reverse clonal expansion and prevent continued genotoxic stress to the overlying premalignant cells [9]. Furthermore, only dermabrasion (i.e., sanding the skin deep into the dermis) has been proven to be effective [10].

Therefore, we proposed that a stromal 'wounding' response to cosmetic NAFL therapies can prevent skin carcinogenesis or delay tumorigenesis. This proposed approach is related to the growing appreciation for the role of the tissue microenvironment (e.g., extracellular matrix (ECM) remodeling/realignment and inflammation) and other stromal cells (e.g., fibroblasts, macrophages, and endothelial cells) in tumor development. Wound healing responses in the stroma induced by NAFL may correct the stromal alterations and suppress carcinogenesis. In particular, we hypothesized that NAFL could be an alternative modality for stromal treatment during early tumorigenesis of epithelial cancer. This study aimed to investigate the potential suppression effect of NAFL irradiation in early cancer growth using syngeneic mouse tumor models. We used numerical simulation to understand thermal injury after NAFL irradiation. Furthermore, we examined a possible normalization mechanism of tumor growth biochemically using cytokine analysis.

II. MATERIALS AND METHODS

2.1 Development of subcutaneous syngeneic mouse tumor models

This study was approved by the Institutional Animal Care and Use Committee Board of the Gwangju Institute of Science and Technology (GIST-2016-13). Five-week-old C57BL/6 and BALB/c mice were acclimatized for 1 week prior to use in the study (Fig. 1A). The hair of the right flank was shaved under anesthesia with a zoletil/xylazine mixture in saline solution (60/10 mg/kg body weight). SL4-DsRed cancer cells (1×10^5 cells) were suspended in 50 μL of phosphate buffered saline and injected into the right flank of C57BL/6 mice. Similarly, the same number of CT26 cancer cells was injected into the right flank of BALB/c mice. Then, each mouse was randomly categorized into two groups: irradiation group (n = 5) and control group (n = 6).

2.2 Non-ablative fractional laser (NAFL) irradiation of syngeneic mouse tumor models

NAFL was used to irradiate the skin 24 hours after cancer cell injection. A thulium fiber based NAFL system (1927 nm, Lavieen, WONTECH, Daejeon, South Korea) was used for the experiments. Under anesthesia, the irradiated group mice received a 70 mJ/spot on the right flank, which included the previous cancer cell-injected area (Fig. 1B). The handpiece of the NAFL system was focused on the right flank of the mouse. Thirteen by thirteen, multiple irradiation spots were generated by point-by-point scanning on 9 mm×9 mm sized rectangular field on the mouse skin. Each irradiation spot was irradiated with a 10 W thulium laser beam for the duration of 7 milliseconds. Compared with the irradiation group, the control group did not receive NAFL irradiation. Tumor growth of both groups of mice were closely followed up afterwards.

2.3 In vivo and ex vivo fluorescence imaging of implanted SL4-DsRed tumor cell

Fluorescence imaging was performed before and after NAFL irradiation. Prior to the NAFL irradiation, SL4-DsRed tumor-bearing mice were imaged to check the location of cancer cells with an optical imaging system (IVIS Luminar II, Caliper Life Sciences, Hopkinton, MA, USA) (Fig. 1C, D). During the imaging, excitation (535 nm) and emission (580 nm) filters were applied to find specific fluorescence signals from cancer cells. After NAFL irradiation, the skin layer was excised from the tumor model to confirm the viability of cancer cells (Fig. 1E, F). The fluorescence signal was investigated by using an upright microscope (CX41, Olympus, Japan) with a fluorescence filter module (DMG 2, Olympus, Japan) (Fig. 1G, H). An LED light source (525 nm) was used as an excitation light source (Touch bright, Live Cell Instrument, Korea) with exposure time of 90 milliseconds.

2.4 Numerical simulation study of temperature distribution after NAFL irradiation

To determine the spatial extent of thermal injury to the skin after NAFL irradiation, the skin tissue of interest was modeled as a slab of $4.5\times4.5\times1$ mm^3 (Fig. 2A, B). Nine cylindrical objects were arrayed in a 3-by-3 fashion to represent the NAFL irradiated spots. The dimensions of each cylindrical object were chosen to reflect the actual NAFL irradiation condition (diameter: 200 μm, height: 250 μm). The center-to-center interval of adjacent cylindrical

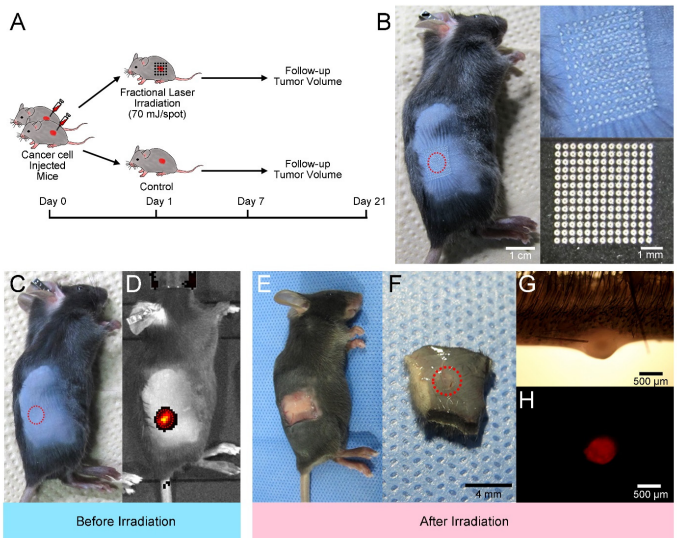

FIG. 1. Non-ablative fractional laser (NAFL) irradiation of the syngeneic mouse tumor model. (A) Schematic illustration of the experiment. Cancer cell-injected mice were divided into irradiation and control groups. NAFL (70 mJ/spot) was applied to the irradiation group, whereas no irradiation was delivered to the control group. The serial tumor volume was followed to measure the therapeutic efficacy of NAFL irradiation from day 7 to 21; (B) NAFL irradiated mouse. Left: NAFL irradiated SL4-DsRed tumor model mouse (red-dotted circle: cancer cell-injected site). Right upper: Magnified image of the flank lesion. Right lower: Array of NAFL irradiated spots on black paper; (C) Photo image shows no significant elevated lesion one day after cancer cell injection (red-dotted circle: cancer cell injection site); (D) Fluorescence image from an optical imaging system; (E) Excised flank skin from an SL4-DsRed injected mouse right after NAFL irradiation; (F) Magnified image of the excised tissue; (G) White light image of the excised tissue slice. (H) Fluorescence image of the excised tissue slice.

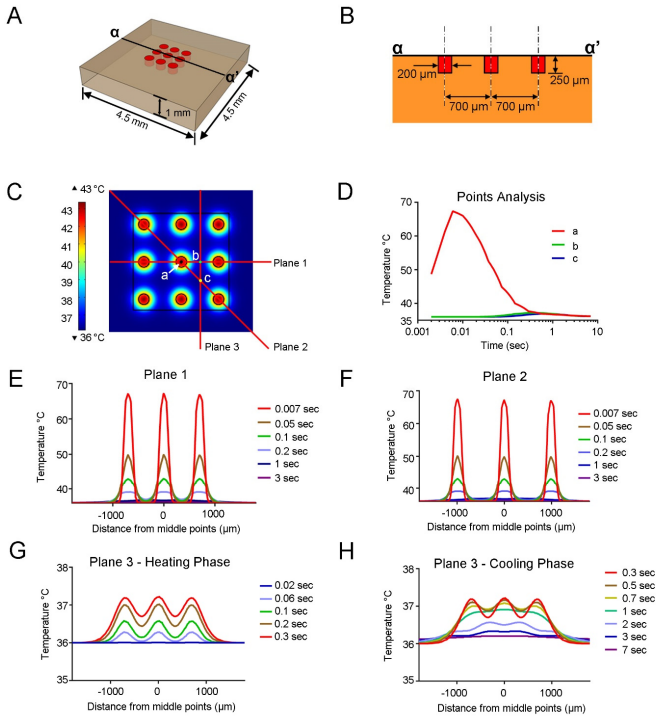

FIG. 2. Numerical simulation of non-ablative fractional laser (NAFL) irradiation to skin tissue. (A) 3D image of the tissue model for numerical simulation; (B) Cross-cut image of the 3D tissue model with plane α–α' in Figure 2A; (C) Three representative spots and three image planes for temporal and spatial analysis; (D) Temporal distribution of the temperature changes at points a, b, and c; (E, F) Spatial distribution of the temperature in the tissue model along Plane 1 (E) and Plane 2 (F); (G, H) Spatial distribution of the temperature during heating (G) and cooling (H) in the tissue model along plane 3.

objects was 700 μm. It was assumed that 10 W laser light was delivered to each object for 0.007 seconds. The photothermal analysis of the skin tissue model was performed using commercial software (Comsol Multiphysics Version 5.1, COMSOL Inc., CA, USA). Eq. (1) is the governing equation for heat transfer through the skin with laser irradiation:

$$\rho C_p \frac{\partial T}{\partial t} = \nabla \bullet \left(k \nabla T \right) + Q_{bio} + Q_{laser} \tag{1}$$

This equation is the general form of the heat diffusion equation where T, ρ, C_p, k, t, Q_{bio}, and Q_{laser} are the temperature of tissue, density, specific heat, thermal conductivity, time, non-directional heat exchange by blood perfusion, and heat source by laser absorption into the skin, respectively. Q_{bio} is based on the Eq. (2), which named as Pennes bioheat equation [11]:

$$Q_{bio} = \rho_b C_b \omega_b \left(T - T_b \right) + Q_m \tag{2}$$

with blood density ρ_b, blood specific heat capacity C_b, blood perfusion rate ω_b, blood temperature T_b, and metabolic heat generation Q_m [11, 12]. The absorbed energy into the skin from a high power laser can be regarded as a heat source. This can be written in differential form of the light intensity I as Eq. (3):

$$\partial I / \partial z = \alpha \left(T \right) I \approx \alpha I = Q_{laser} \tag{3}$$

where $\alpha(T)$ is a temperature-dependent absorption coefficient and I is the light intensity. In Eq. (3), the Beer-Lambert law was simplified considering the absorption coefficient. We used the absorption coefficient of 5 cm^{-1} corresponding to the wavelength of the laser used in the simulation [13, 14]. All thermal properties of the skin and blood used in the simulation are based on previous papers [15-19] and are listed in Table 1.

The initial tissue and blood temperatures were set to be 36ºC and 37ºC, respectively. Results of numerical simulation were displayed as a spatial and temporal distribution of temperature throughout the tissue model. The temperature distribution was calculated along three representative cutting planes 125 μm below the surface (Fig. 2C). Three representative spots within the tissue model were selected and used to describe temperature changes over time.

TABLE 1. Thermal properties of the skin and blood

	Skin	Blood
Thermal conductivity, k [W/m·K]	0.379	-
Density, ρ [kg/m^3]	1118	1057
Heat capacity, C [J/kg·K]	3634	3600
Blood perfusion rate, ω_b [sec^{-1}]	0.00117	-
Metabolic heat source, Q_m [W/m^3]	631	-

2.5 Cell culture

SL4-DsRed and CT26, two murine colon cancer cell lines, were cultured to make syngeneic mouse tumor models. SL4-DsRed was kindly provided by the Edwin L. Steel Laboratory (Massachusetts General Hospital and Harvard Medical School, MA, USA) and CT26 was obtained from the ATCC (Manassas, VA, USA). SL4-DsRed cells were cultured in Dulbecco's modified Eagle's Medium/Ham's F-12 (DMEM/F12) 1:1 medium supplemented with L-glutamine and 2.438 g/L NaHCO3, 10% fetal bovine serum (FBS), 1% penicillin/streptomycin solution. CT26 cells were cultured in DMEM, 10% FBS, and 1% penicillin/streptomycin solution. All media and reagents were purchased from Gibco (Invitrogen Corporation, Grand Island, NY, USA).

2.6 Tumor volume changes measurements

Tumor sizes of each mouse were measured by calipers 7 days after cancer cell injection and twice a week subsequently. Tumor volumes (TVs) based on the caliper measurement were calculated with Eq. (4) by assuming an ellipsoid shape [20]:

$$\mathrm{TV} = \frac{4}{3} \times \pi \times \frac{\mathrm{length}}{2} \times \frac{\mathrm{width}}{2} \times \frac{\mathrm{height}}{2} \tag{4}$$

Follow-up measurements were terminated when the mean TV (MTV) of each group reached 1000 mm^3 or if there was ulceration in the tumors.

2.7 Cytokine level measurement

Irradiation and control SL4-DsRed tumor-bearing C57BL/6 mice were sacrificed at days 1, 7, and 14. At each time point, three mice per each group were used for enzyme-linked immunosorbent assay (ELISA). Blood was collected by cardiac puncture and then serum was harvested using centrifugation. The levels of interferon (IFN)-γ, interleukin (IL)-1β, tumor necrosis factor (TNF)-α, and transforming growth factor (TGF)-β were measured using ELISA kits (eBioscience, San Diego, CA, USA). The absorbance was measured at 450 nm in an ELISA reader (SpectraMax, Molecular Devices, Sunnyvale, CA, USA).

2.8 Statistical analysis

Mann-Whitney U tests were used to compare TVs between the NAFL irradiation group and the control group. All statistical evaluations were performed using SPSS (version 20, SPSS Inc., Chicago, IL, USA).

III. RESULTS

3.1 Optical imaging of SL4-DsRed implanted tumor model

After 24 hours from cancer cell injection, the elevated skin lesion became flat and looked similar to the normal adjacent skin tissue (Fig. 1C). Fluorescence images showed focal signal intensity in the right flank area, where the cancer cell injection site was confirmed by the presence of DsRed fluorescence (Fig. 1D).

The irradiated skin area was excised from SL4-DsRed tumor mouse right after NAFL irradiation (Fig. 1E). In the magnified view, the focal whitish lesion was observed on the inner wall of skin layer (Fig. 1F). After tissue slicing, optical microscope images revealed a focal protrusion region on the subcutaneous fat layer (Fig. 1G). Fluorescence images also showed focal signal at the same location with high contrast compared to the adjacent tissue (Fig. 1H). This implicates the existence of viable SL4-DsRed cells after NAFL irradiation within the subcutaneous fat layer of the skin.

3.2 Temperature distribution of the NAFL irradiation skin tissue model

To estimate thermal injury from NAFL irradiation, nine laser irradiation spots were made on the tissue model (Fig. 2A). Numerical simulation experiment results showed heat transfer from irradiation spots to the adjacent tissue (Fig. 2C). Three planes (1, 2 and 3) and three points (a, b, and c) were selected for the temperature analysis. The temporal changes in temperature at these three representative points showed the highest temperature rise at the center of the NAFL irradiation spot, with lower temperature changes in the areas between the irradiation spots (Fig. 2D). The spatial temperature distribution of plane 1 and plane 2 showed three highest temperature peaks on the NAFL irradiation spot (Fig. 2E, F). The highest temperature was observed at the center of the irradiation spot, reaching 67.2°C in 0.007 seconds, which suggested that the highest temperature was reached when the NAFL irradiation ended. In plane 3, the highest temperature was 37.2°C at 0.3 seconds after NAFL irradiation at the central points between the two adjacent

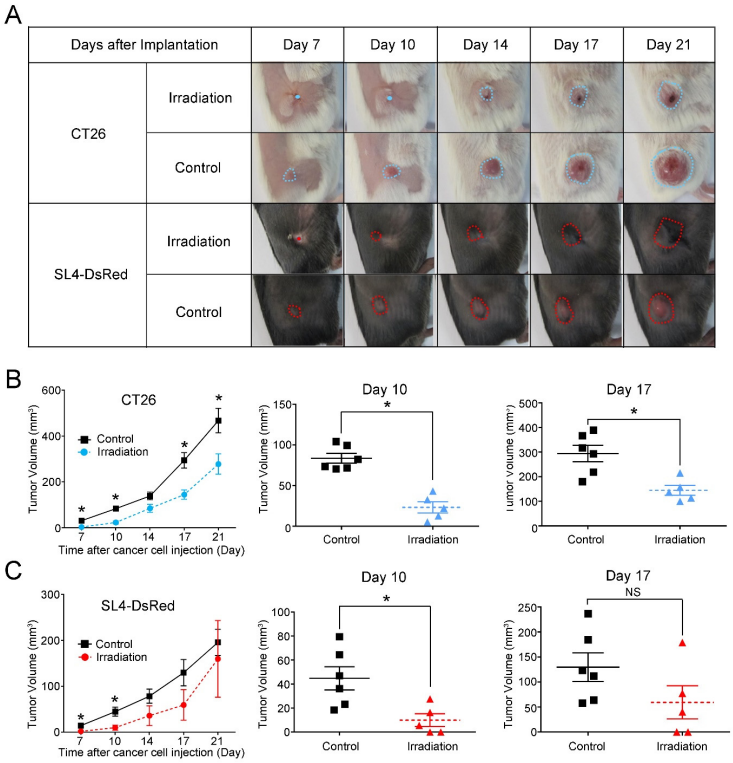

FIG. 3. Tumor volume changes in syngeneic mouse tumor models. (A) Representative images of serial tumor volume (TV) changes during the follow-up periods. The blue- and red-dotted lines show the contour of the tumor. A single dot means no significant tumor lesion at the site; (B) In the CT26 implanted tumor model, the irradiation group (blue-dotted line) had smaller mean TVs (MTVs) than the control group (black solid line). On day 10 and day 17 after CT26 injection there is a statistically significant difference in MTVs between the irradiation and control groups; (C) In the SL4-DsRed tumor model, the irradiation group (red-dotted line) had smaller MTVs than the control group (black solid line). This difference in TV between the irradiation and control groups was observed on day 10 but not on day 17. Noticeably, 2 of the 5 SL4-DsRed cancer cell-injected mice had shown no significant tumor growth until 90 days after cancer cell injection. An asterisk (*) indicates statistical significance < 0.05 while NS indicates no significance. All results are presented as mean ± SEM.

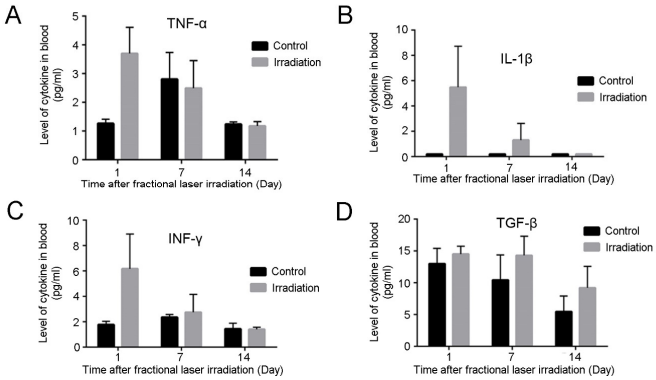

FIG. 4. Cytokine analysis of SL4-DsRed tumor models. Enzyme-linked immunosorbent assays (ELISA) were performed to analyze the levels of the cytokines (A) TNF-α, (B) IL-1β, (C) IFN-γ, and (D) TGF-β. TNF-α, IL-1β, and IFN-γ levels were elevated on day 1 after NAFL irradiation. TGF-β did not show any significance changes during the experimental period. All results are shown as mean ± SEM.

NAFL irradiation spots (Fig. 2G - Heating phase). After 0.3 seconds, the temperature peak became smoother within the adjacent tissue (Fig. 2H - Cooling phase).

3.3 Growth suppression of the tumor by NAFL irradiation

All control group mice showed persistent tumor growth throughout the time course (Fig. 3A). There were no significant differences in body weight between the irradiation group and the control group in both mouse tumor models. In the CT26 model, the irradiation group showed a smaller MTV than the control group after the cancer cell injection (Fig. 3B). Tumor measurements on day 10 and 17 showed statistically significantly smaller MTVs in the irradiation group than the control group. This difference was maintained for 21 days after the cancer cell injection. Similar results were observed in the SL4-DsRed model (Fig. 3C), where the irradiation group also showed a smaller MTV than the control group. Notably, two out of five irradiated C57BL/6 mice with SL4-DsRed cancer cell injection had no measurable tumor growth until 90 days after NAFL.

3.4 An inflammatory reaction was induced by NAFL irradiation on day 1

Both TNF-α and IL-1β levels were acutely elevated 1 day after NAFL irradiation (Fig. 4A, B). After day 7, the level of TNF-α showed no significant difference between the irradiation and control groups. For IL-1β, the rapid elevation in the irradiation group on day 1 diminished subsequently. On day 14, IL-1β was undetectable in both irradiation and control groups. IFN-γ level was elevated in the irradiation group compared with the control group on day 1 and it gradually declined after day 7 (Fig. 4C). While all three cytokines showed an elevated tendency in the irradiation group on day 1 after NAFL irradiation, there was no obvious difference in TGF-β between the two groups (Fig. 4D).

IV. DISCUSSION

We demonstrated the tumor growth suppression effect of NAFL with two syngeneic mouse tumor models. To our knowledge, this is the first report on the use of NAFL as an anticancer stromal treatment modality. We used a thulium fiber based NAFL system for these experiments. The thulium fiber laser offers higher efficiency, improved beam quality, and inherent fiber optic beam delivery, which enables easy coupling to other fiber optics [21]. The wavelengths of a thulium fiber laser (1927 nm) have a high absorption coefficient in water [22] that leads to a relatively shallow penetration depth up to 200 μm from the tissue surface [23]. Therefore, it is widely used for superficial skin rejuvenation [24-26]. In our study with two strains of syngeneic tumor mice (i.e. C57BL/6 and BALB/c), the average thickness of the epidermis and dermis layers were over 200 μm [27]. Laser irradiation cannot cause direct damage to cancer cells, and thus we investigated the secondary effects from laser irradiation.

The dose of delivered energy to the tissue by laser irradiation could be critical. We applied 70 mJ/spot of NAFL energy in this preclinical experiment based on previous reports [28]. This is a dose higher than that used clinically (5-20 mJ/spot) [29, 30]. However, because of the characteristics of NAFL, it was still confined within the dermis layer and caused molecular changes. Instead of adjusting the laser parameters, we tried changing the number of cancer cells. We increased the number of cancer cells injected into the mouse flank from 100,000-500,000 cells per site (Fig. 5). In this supplemental study, we obtained outcomes similar to the previous one. The irradiation groups had a smaller MTV than that of the control groups in both tumor models. However, the suppression effect of tumor growth was lost in an earlier stage than that in the 100,000 cell-injected experiment. These results suggested that NAFL irradiation can interfere with early tumorigenesis.

We confirmed the typical characteristics of NAFL, which

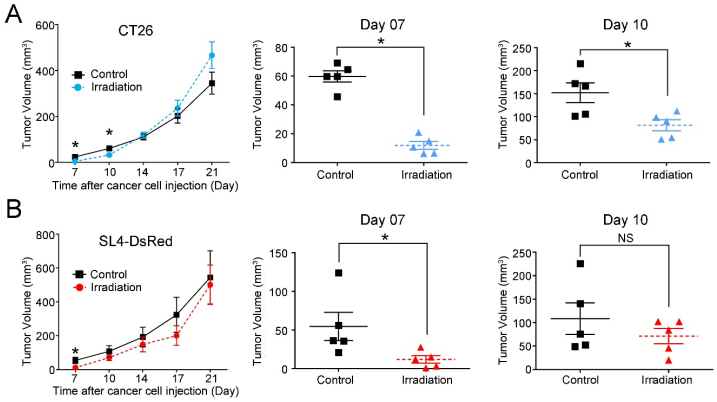

FIG. 5. Tumor volume changes of the tumor-bearing mouse model after injection of an increased number of cancer cells. Half a million cancer cells were injected into each mouse. (A) In the CT26 implanted tumor model, the irradiation group (blue-dotted line) had a smaller mean tumor volume (MTV) than the control group (black solid line). Day 7 and day 10 after CT26 injection there was a statistically significant difference in MTV between the irradiation and control group; (B) In the SL4-DsRed tumor model, the irradiation group (red-dotted line) had a smaller MTV than the control group (black solid line). This difference in MTV between the irradiation and control groups was observed on day 7 but not on day 10. Representative images of serial MTV change during the follow-up period. An asterisk (*) indicates statistical significance < 0.05 while NS means no significance. All results are presented as mean ± SEM.

results in microscopic thermal wounds on the irradiation site and spares interstitial tissue surrounding each irradiation spot. The numerical simulation results showed the highest temperature rise, to 67.2°C, at the irradiated spots immediately after NAFL irradiation. However, the temperature of the irradiated spots decreased below 40°C within 0.2 seconds after irradiation. In the adjacent tissue region between the irradiation spots (Plane 3), temperature changes were less than 2°C (from 36.0°C to 37.22°C). To simplify the numerical simulation, we assumed that irradiation was applied simultaneously to all spots. However, the actual laser irradiation was done in consecutive order with point-by-point scanning with 2.3 milliseconds interval. Thus the temperature change at the adjacent tissue of the irradiation spot would be less in the experiment than the simulation. Therefore, our numerical simulation can mimic the severest condition by the NAFL irradiation to tissue. Due the use of a severe condition for simulation, the adjacent tissue temperature showed a relatively small change.

Using the red fluorescent protein (DsRed) in the SL4 murine colon cancer cell line, we identified the cancer cell accumulation site before and after NAFL irradiation (Fig. 1C-H). They were properly located in the subcutaneous fatty layer and emitted red light with a well-margined round shape. This focal accumulation of cancer cells was seen in all SL4-DsRed cancer cell-injected animals. Although the CT26 cancer cells did not have a fluorescence marker, we could still observe a focal whitish accumulated lesion in the inner wall of the excised skin layer from BALB/c mice.

The molecular mechanism of NAFL therapy is associated with an inflammatory infiltrate and reorganization of the dermal matrix [2, 31]. Our ELISA results demonstrated that NAFL irradiation induces proinflammatory cytokines, TNF-α and IL-1β (Fig. 4A, B). These results are consistent with those in the previously reported literature [28]. Our results showed an early elevation of IFN-γ levels a day after NAFL irradiation. The levels of IFN-γ increased in the experimental group relative to that of the control group. However, the growth suppression effect was lost over time. The statistical difference disappeared after day 14 in the SL4-DsRed model (Fig. 3C). In the CT26 model, the significant difference between the irradiation and control groups was maintained until day 21 (Fig. 3B). Further time points were not assessed because of the presence of central ulceration on the tumor in several mice.

IFN-γ has a critical role in host protection against primary and transplanted tumors [32]. A previous study showed that IFN-γ induced by surgical wounds suppresses tumor growth in a syngeneic mouse tumor model [33]. Similar to our results, the growth suppression effect was lost over time and rapid tumor regrowth occurred. The authors explained the reason for this loss of effect as TGF-β activity [34]. Because of the antagonistic effect of TGF-β on IFN-γ, the tumor showed regrowth over time. TGF-β is known to have dual functions, both as a tumor suppressor and a tumor promoter [35, 36]. In the early tumor stages, TGF-β suppresses tumor growth through genetic control and induces apoptosis of tumor cells. However, as the tumor develops, tumor cells frequently become resistant to TGF-β mediated growth suppression and respond instead with increased migration, invasion, and metastasis.

To mimic early stage tumorigenesis, we irradiated mice with NAFL 1 day after subcutaneous cancer cell inoculation. We observed an elevation of cytokine levels immediately after NAFL irradiation in some of the samples from the SL4-DsRed model (n = 3). After controlled injury from NAFL

irradiation, a local inflammatory change could regulate the early stage of tumorigenesis in a minimally invasive manner.

The limitation of this study was that the tumor model was made on ectopic site. We inoculated colon cancer cell into the subcutaneous area of the right flank of a mouse. Different organ environments can affect the sensitivity of tumor cells to cancer treatment [37]. Future experiments with orthotopic tumor models or genetically engineered tumor models will strengthen the finding of cancer therapeutic effect of NAFL irradiation.

V. CONCLUSION

Seeking a novel use of laser treatment, we demonstrated that non-ablative fractional laser (NAFL) irradiation suppresses early stage tumor growth with minimal thermal damage to adjacent tissues with two syngeneic mouse tumor models. Interestingly, some mice did not show tumor growth, which means cure from cancer cell implantation. Minimally damaged tissue evokes inflammatory changes, and elevated inflammatory cytokines may suppress early tumorigenesis. This tumor suppression effect of NAFL was more prominent when the number of the injected cancer cell was small. Therefore, stromal NAFL irradiation has the potential to be an alternative, minimally invasive cancer therapeutic modality for early stages of tumorigenesis.

ACKNOWLEDGMENT

The authors thank Mai Thi-Quynh Duong and Jin Hai Zheng (from Department of Nuclear Medicine, Chonnam National University Medical School and Hwasun Hospital, Jeonnam, Korea) for experimental help. This work was supported by the Korea Foundation for Cancer Research (KFCR-2014-003), GIST Research Institute (GRI) by GIST in 2016, Biomedical Integrated Technology Research Project through a grant provided by GIST in 2016, the GIST-Caltech Research Collaboration Project through a grant provided by GIST in 2016, Engineering Research Center (No.2011-0030075) of the National Research Foundation (NRF), and by the Korean government (MEST) (NRF-2011-0019633, NRF-2016R1A2B4015381).

REFERENCES

1. J. Lipozencic and Z. Bukvic Mokos, "Dermatologic lasers in the treatment of aging skin," Acta Dermatovenerol Croat. **18**, 176-180 (2010).
2. H. J. Laubach, Z. Tannous, R. R. Anderson, and D. Manstein, "Skin responses to fractional photothermolysis," Lasers Surg. Med. **38**, 142-149 (2006).
3. R. G. Geronemus, "Fractional photothermolysis: current and future applications," Lasers Surg. Med. **38**, 169-176 (2006).
4. K. D. Polder and S. Bruce, "Treatment of melasma using a novel 1,927-nm fractional thulium fiber laser: a pilot study," Dermatol. Surg. **38**, 199-206 (2012).
5. D. F. Spandau, D. A. Lewis, A. K. Somani, and J. B. Travers, "Fractionated laser resurfacing corrects the inappropriate UVB response in geriatric skin," J. Invest Dermatol. **132**, 1591-1596 (2012).
6. J. Gye, S. K. Ahn, J. E. Kwon, and S. P. Hong, "Use of fractional CO2 laser decreases the risk of skin cancer development during ultraviolet exposure in hairless mice," Dermatol. Surg. **41**, 378-386 (2015).
7. R. R. Anderson, "Lasers for dermatology and skin biology," J. Invest Dermatol. **133**, E21-23 (2013).
8. C. P. Barham, R. L. Jones, L. R. Biddlestone, R. H. Hardwick, N. A. Shepherd, and H. Barr, "Photothermal laser ablation of Barrett's oesophagus: endoscopic and histological evidence of squamous re-epithelialisation," Gut. **41**, 281-284 (1997).
9. R. L. Konger, Z. Xu, R. P. Sahu, B. M. Rashid, S. R. Mehta, D. R. Mohamed, S. C. DaSilva-Arnold, J. R. Bradish, S. J. Warren, and Y. L. Kim, "Spatiotemporal assessments of dermal hyperemia enable accurate prediction of experimental cutaneous carcinogenesis as well as chemopreventive activity," Cancer Res. **73**, 150-159 (2013).
10. L. M. Field, "The superiority of dermabrasion over laser abrasion in the prophylaxis of malignant and premalignant disease," Dermatol. Surg. **33**, 258-259 (2007).
11. H. H. Pennes, "Analysis of tissue and arterial blood temperatures in the resting human forearm," J. Appl. Physiol. **1**, 93-122 (1948).
12. T. L. Bergman, A. S. Lavine, F. P. Incropera, and D. P. DeWitt, "*The Bioheat Equation*," *in Fundamentals of Heat and Mass Transfer*. 183-187 (Wiley, 2011).
13. A. N. Bashkatov, E. A. Genina, V. I. Kochubey, and V. V. Tuchin, "Optical properties of human skin, subcutaneous and mucous tissues in the wavelength range from 400 to 2000 nm," J. Phys. D: Appl. Phys. **38**, 2543-2555 (2005).
14. A. N. Bashkatov, É. A. Genina, V. I. Kochubey, and V. V. Tuchin, "Optical properties of the subcutaneous adipose tissue in the spectral range 400-2500 nm," Opt. Spectrosc. **99**, 836-842 (2005).
15. D. Ratovoson, F. Jourdan, and V. Huon, "A study of heat distribution in human skin: use of Infrared Thermography," EPJ Web Conf. **6**, 21008 (2010).
16. Z. Ostrowski, P. Bulinski, W. Adamczyk, and A. J. Nowak, "Modelling and Validation of transient heat transfer processes in human skin undergoing local cooling," Prz. Elektrotechniczny. **91**, 76-79 (2015).
17. J. Z. Wensheng Shen and Fuqian Yang, "Modeling and numerical simulation of bioheat transfer and biomechanics in soft tissue," Math Comput Modell. **41**, 1251-1265 (2005).
18. S. M. Lin and C. Y. Li, "Analytical solutions of non-Fourier bio-heat conductions for skin subjected to pulsed laser heating," Int. J. Therm Sci. **110**, 146-158 (2016).
19. C. M. Collins, M. B. Smith, and R. Turner, "Model of local temperature changes in brain upon functional activation," J. Appl. Physiol. **97**, 2051-2055 (2004).
20. J. Sapi, L. Kovacs, D. A. Drexler, P. Kocsis, D. Gajari, and Z. Sapi, "Tumor Volume Estimation and Quasi-Continuous Administration for Most Effective Bevacizumab Therapy," PLoS. One. **10**, e0142190 (2015).

21. H. Z. Alagha and M. Gulsoy, "Photothermal ablation of liver tissue with 1940-nm thulium fiber laser: an ex vivo study on lamb liver," J. Biomed Opt. **21**, 15007 (2016).
22. A. B. Niwa Massaki, S. Eimpunth, S. G. Fabi, I. Guiha, W. Groff, and R. Fitzpatrick, "Treatment of melasma with the 1,927-nm fractional thulium fiber laser: a retrospective analysis of 20 cases with long-term follow-up," Lasers Surg. Med. **45**, 95-101 (2013).
23. M. Rieken and A. Bachmann, "Laser treatment of benign prostate enlargement--which laser for which prostate?," Nat Rev. Urol. **11**, 142-152 (2014).
24. P. Ghasri, S. Admani, A. Petelin, and C. B. Zachary, "Treatment of actinic cheilitis using a 1,927-nm thulium fractional laser," Dermatol. Surg. **38**, 504-507 (2012).
25. L. Miller, V. Mishra, S. Alsaad, D. Winstanley, T. Blalock, C. Tingey, J. Qiu, S. Romine, and E. V. Ross, "Clinical evaluation of a non-ablative 1940 nm fractional laser," J. Drugs Dermatol. **13**, 1324-1329 (2014).
26. J. A. Brauer, D. H. McDaniel, B. S. Bloom, K. K. Reddy, L. J. Bernstein, and R. G. Geronemus, "Nonablative 1927 nm fractional resurfacing for the treatment of facial photopigmentation," J. Drugs Dermatol. **13**, 1317-1322 (2014).
27. K. Calabro, A. Curtis, J. R. Galarneau, T. Krucker, and I. J. Bigio, "Gender variations in the optical properties of skin in murine animal models," J. Biomed Opt. **16**, 011008 (2011).
28. J. S. Orringer, L. Rittie, D. Baker, J. J. Voorhees, and G. Fisher, "Molecular mechanisms of nonablative fractionated laser resurfacing," Br. J. Dermatol. **163**, 757-768 (2010).
29. K. D. Polder, A. Harrison, L. E. Eubanks, and S. Bruce, "1,927-nm fractional thulium fiber laser for the treatment of nonfacial photodamage: a pilot study," Dermatol. Surg. **37**, 342-348 (2011).
30. E. T. Weiss, J. A. Brauer, R. Anolik, K. K. Reddy, J. K. Karen, E. K. Hale, L. A. Brightman, L. Bernstein, and R. G. Geronemus, "1927-nm fractional resurfacing of facial actinic keratoses: a promising new therapeutic option," J. Am. Acad. Dermatol. **68**, 98-102 (2013).
31. D. B. Vasily, M. E. Cerino, E. M. Ziselman, and S. T. Zeina, "Non-ablative fractional resurfacing of surgical and post-traumatic scars," J. Drugs Dermatol. **8**, 998-1005 (2009).
32. H. Ikeda, L. J. Old, and R. D. Schreiber, "The roles of IFN gamma in protection against tumor development and cancer immunoediting," Cytokine Growth Factor Rev. **13**, 95-109 (2002).
33. Y. M. Ma, T. Sun, Y. X. Liu, N. Zhao, Q. Gu, D. F. Zhang, S. Qie, C. S. Ni, Y. Liu, and B. C. Sun, "A pilot study on acute inflammation and cancer: a new balance between IFN-gamma and TGF-beta in melanoma," J. Exp. Clin. Cancer Res. **28**, 23 (2009).
34. S. B. Jakowlew, "Transforming growth factor-beta in cancer and metastasis," Cancer Metastasis Rev. **25**, 435-457 (2006).
35. I. P. Witz, "Yin-yang activities and vicious cycles in the tumor microenvironment," Cancer Res. **68**, 9-13 (2008).
36. I. P. Witz, "Tumor-microenvironment interactions: dangerous liaisons," Adv. Cancer Res. **100**, 203-229 (2008).
37. C. Wilmanns, D. Fan, C. A. O'Brian, C. D. Bucana, and I. J. Fidler, "Orthotopic and ectopic organ environments differentially influence the sensitivity of murine colon carcinoma cells to doxorubicin and 5-fluorouracil," Int. J. Cancer. **52**, 98-104 (1992).